

### 6.3 Effect of Particle size

Five different particle sizes of each of the sorbents, ranging from 0.18mm to 0.71mm were utilized to investigate the influence of the adsorbent particle size for Cr(VI) removal. It is observed from the smooth and continuous curves (figures 6.11 and 6.12) that 0.18mm and 0.42mm particle sizes of TTCNS and TAINS registered enhanced sorption capacity. This is confirmed by the data tabulated in tables 6.1 and 6.2 where the values 26.8 mg/g and 85.88 mg/g showed maximum for the optimum particle sizes. Hence the experiments pertaining to other parameters were carried out employing 0.18mm TTCNS and 0.42mm TAINS.

**Table 6.1 Effect of Particle size (TTCNS)**

Time (min)	Amount Adsorbed (mg/g)				
	0.18 mm	0.24 mm	0.30 mm	0.42 mm	0.71 mm
0	0	0	0	0	0
5	15.1	20.9	20.9	15.5	14.8
10	23.4	22.6	21.2	16.1	14.8
15	23.6	23.2	21.4	16.3	12.0
20	23.8	23.4	21.5	16.7	12.0
25	25.8	23.8	21.8	16.9	11.3
30	26.8	24.9	22.2	18.5	11.2
35	27.2	25.1	23.8	18.7	11.2
40	27.0	25.0	23.5	18.9	11.2

Metal ion concentration:11 ppm; Adsorbent dose:200 mg; pH:1.78; Temperature: 303K.

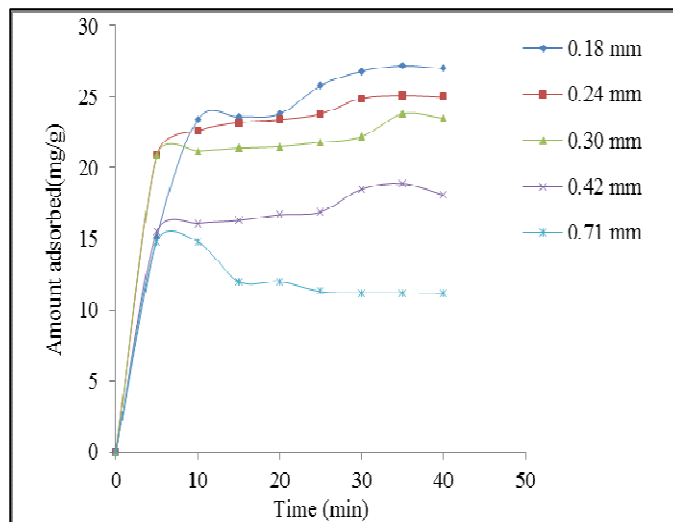


**Figure 6.11 Effect of Particle size (TTCNS)**

**Table 6.2 Effect of Particle size (TAINS)**

Time (min)	Amount Adsorbed (mg/g)				
	0.18 mm	0.24 mm	0.30 mm	0.42 mm	0.71 mm
0	0	0	0	0	0
5	37.39	51.00	60.6	63.18	73.51
10	42.98	52.66	70.05	64.47	73.93
15	44.76	55.60	70.91	67.90	77.77
20	45.11	58.20	72.63	85.88	80.76
25	47.28	58.20	72.63	88.87	83.32
30	50.72	60.20	76.50	89.30	84.60
35	52.43	61.80	79.94	93.56	85.29
40	53.72	58.80	81.23	99.54	87.16

Metal ion concentration: 11 ppm; Adsorbent dose: 150 mg; pH: 1.98; Temperature: 303K

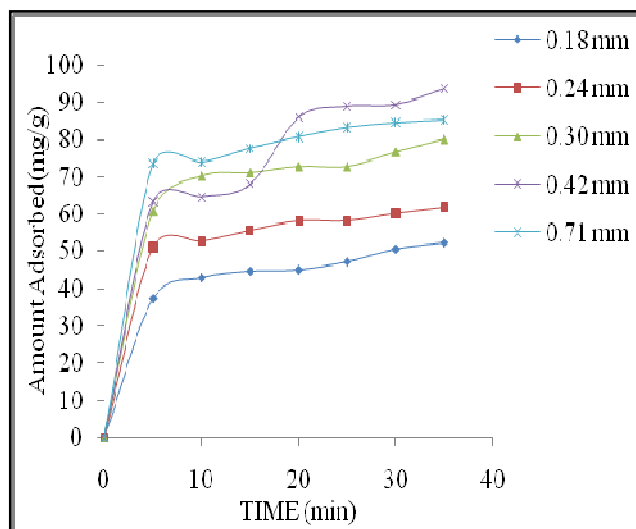


**Figure 6.12 Effect of Particle size (TAINS)**

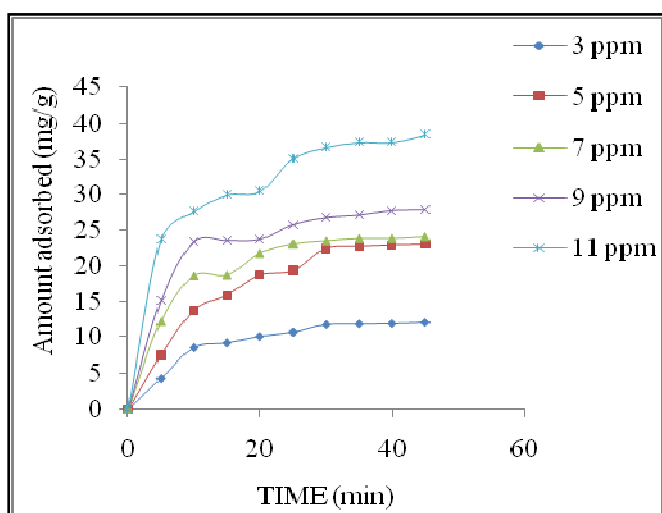
#### 6.4 Effect of Contact time and Initial concentration

At 30 minutes, higher amounts of Cr(VI) was adsorbed onto TTCNS and the values were 11.85, 22.8, 23.8, 27.2 and 37.4 mg/g for initial concentrations of 3,5,7,9 and 11 ppm respectively (Table 6.3). Similarly 15 minutes equilibrium time was observed for Cr(VI) sorption onto TAINS, as evident from table 6.4. As the contact time increases, the amount of Cr(VI) getting adsorbed increases, but at a particular point of time, the system attains equilibrium. The percentage removal of Cr(VI) increased upto 30 minutes and 15 minutes for TTCNS and TAINS respectively and after that no further rise was recorded and hence these time profiles were considered optimum<sup>284</sup>.

**Table 6.3 Effect of Contact time and Initial concentration (TTCNS)**

Time(min)	Amount adsorbed (mg/g)				
	3 ppm	5ppm	7ppm	9ppm	11ppm
5	4.30	7.50	12.15	15.10	23.8
10	8.50	13.75	18.55	23.40	27.7
15	9.15	15.95	18.65	23.60	30.0
20	10.05	18.75	21.70	23.80	30.5
25	10.65	19.40	23.00	25.85	35.1
30	11.75	22.50	23.45	26.85	36.7
35	11.85	22.80	23.80	27.20	37.4
40	11.90	23.00	23.80	27.85	37.4
45	12.05	23.10	24.05	27.95	38.5

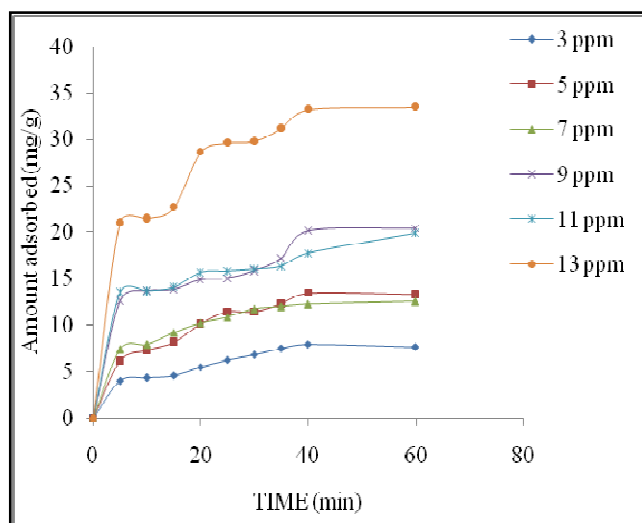
Particle size: 0.18 mm; Adsorbent dose: 200mg; pH: 1.78; Temperature: 303K

**Figure 6.13 Effect of Contact time and Initial concentration (TTCNS)**

**Table 6.4 Effect of Contact time and Initial concentration (TAINS)**

Time(min)	Amount adsorbed mg/g					
	3 ppm	5ppm	7ppm	9ppm	11ppm	13ppm
5	4.03	6.15	7.39	12.65	21.07	13.53
10	4.37	7.29	7.90	13.72	21.47	13.67
15	4.59	8.15	9.18	13.85	22.67	14.07
20	5.49	10.15	10.20	14.92	28.60	15.67
25	6.28	11.44	10.84	15.05	29.60	15.80
30	6.84	11.44	11.73	15.85	29.80	16.00
35	7.51	12.29	11.98	17.18	31.20	16.33
40	7.96	13.44	12.24	20.11	33.20	17.73

Particle size: 0.42 mm; Adsorbent dose: 150 mg; pH: 1.98; Temperature: 303K

**Figure 6.14 Effect of Contact time and Initial concentration (TAINS)**

## 6.5 Effect of Dosage

The variation in doses (50-250mg; 50mg interval) was experimentally verified, wherein a decrease in the amount adsorbed was observed from 54.4 to 52.3 mg/g and 42.9 to 19.7 mg/g (Tables 6.5 & 6.6) when TTCNS dose was increased from 200-250mg and TAINS from 150-200mg respectively. The decrease in amount adsorbed at higher dose may be basically due to electrostatic interactions between the adsorbent particles and interference between the binding sites<sup>285</sup>.

**Table 6.5 Effect of adsorbent dose (TTCNS)**

Time (min)	Amount adsorbed mg/g				
	50 mg	100mg	150 mg	200 mg	250 mg
0	0	0	0	0	0
5	6.1	6.6	15.6	30.2	37.5
10	13.3	11.5	18.8	46.8	43.8
15	15.0	18.8	23.1	47.2	46.6
20	18.1	21.0	22.5	47.6	51.2
25	24.2	24.4	28.5	51.7	51.5
30	24.8	26.9	31.1	53.7	52.2
35	25.1	27.3	47.0	54.4	52.3
40	30.1	27.8	47.9	55.7	52.6
45	30.8	34.5	48.4	55.9	52.7
60	31.3	35.8	48.8	56.1	52.8

Initial metal ion concentration: 11ppm; pH: 1.78; Temperature: 303K

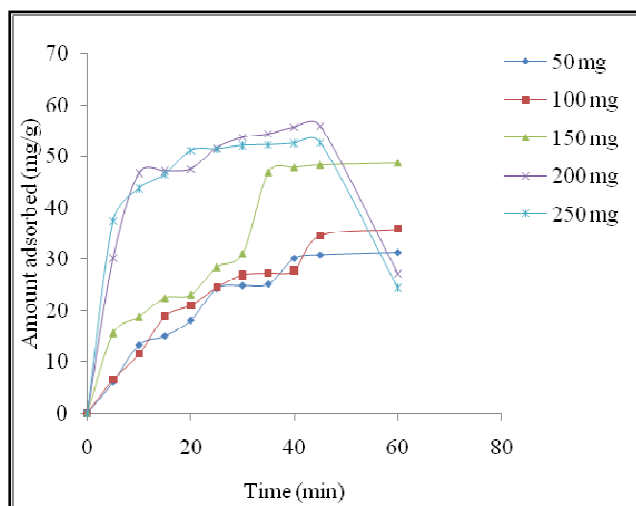


**Figure 6.15 Effect of adsorbent dose (TTCNS)**

**Table 6.6 Effect of adsorbent dose (TAINS)**

Time (min)	Amount adsorbed mg/g				
	50 mg	100 mg	150 mg	200 mg	250 mg
0	0	0	0	0	0
5	18.4	22.4	31.6	31.7	10.0
10	18.7	22.5	32.2	36.9	13.5
15	21.6	24.9	34.0	41.3	17.4
20	22.6	26.1	42.9	45.2	19.7
25	23.2	27.5	44.4	45.8	19.7
30	25.1	29.7	44.7	46.3	22.6
35	26.7	30.2	46.8	47.4	23.2
40	30.1	30.5	49.8	45.3	23.2
60	30.4	30.1	49.6	45.3	22.6

Initial metal ion concentration: 11 ppm; pH: 1.98; Temperature: 303K

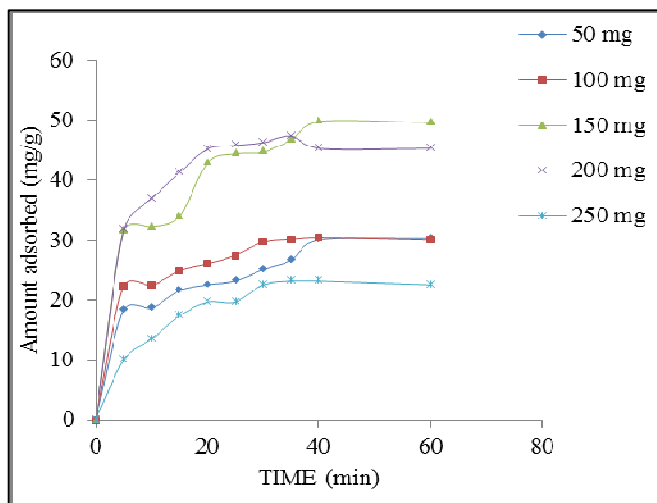


**Figure 6.16 Effect of adsorbent dose (TAINS)**

### 6.6 Effect of pH Cr(VI)

Cr(VI) removal by TTCNS and TAINS was investigated as a function of solution pH over the range 1-8 which is depicted in figures 6.17 and 6.18. Maximum uptake was observed at pH 1.78 and 1.98. At increasing pH environments, a sharp decline in uptake was observed, which is in good agreement with previous reports<sup>184, 167</sup>. The speciation studies of Cr(VI) in aqueous solution shows that  $\text{H}_2\text{CrO}_4$  predominates at pH less than 1.0,  $\text{HCrO}_4^-$  for pH between 1.0 and 6.0 and  $\text{CrO}_4^{2-}$  at pH above 6.2<sup>51</sup>. Adsorption of Cr(VI) at pH 1.78 of TTCNS is due to the electrostatic attraction between the positively charged surface of the adsorbent with  $\text{HCrO}_4^-$  ions. But in highly acidic medium (pH=1.0),  $\text{H}_2\text{CrO}_4$  (neutral form) is the predominant species of Cr(VI). Hence, percentage removal decreased due to the involvement of less number of  $\text{HCrO}_4^-$  anions to the positive surface. At higher pH value, the reduction in adsorption may be due to the dual competition of both  $\text{OH}^-$  and  $\text{CrO}_4^{2-}$  ions to get adsorbed on the surface of the adsorbent among which  $\text{OH}^-$  predominates<sup>254, 239</sup>,

At an initial pH of 2, the surface of TAINS was highly protonated which allows the electrostatic interaction with the predominant anionic form of Cr(VI), (i.e.)  $\text{HCrO}_4^-$ . In the acidic range, these ions have a greater affinity towards the hydrogen ions present on the



surface of TAINS<sup>236</sup>. With the rise in pH from 2.5 to 9.5, the degree of protonation on TAINS surface was observed to reduce gradually and hence the removal was retarded. At higher pH values,  $\text{HCrO}_4^-$  sorption is diminished in preference to  $\text{CrO}_4^{2-}$  and  $\text{OH}^-$  whose prevalence is more<sup>283</sup>.

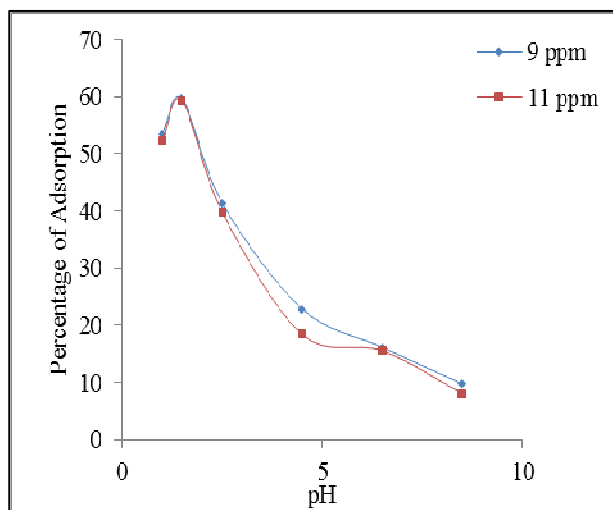


**Figure 6.17 Effect of pH (TTCNS)**

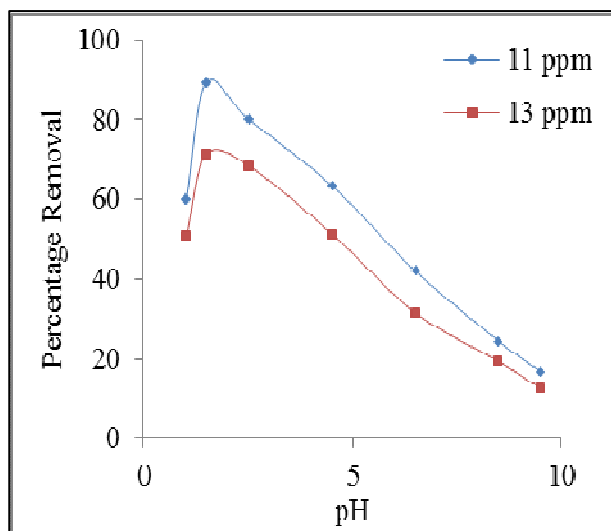


**Figure 6.18 Effect of pH (TAINS)**

## 6.7 Effect of Cations

The influence of sodium, potassium and magnesium on Cr(VI)-TTCNS and Cr(VI)-TAINS systems were carried out at varied concentrations (11-100 ppm) of these cations. The corresponding plots represented in figures 6.19 and 6.20 imply that the influence of these ions on Cr(VI) removal is insignificant. As stated earlier, Cr(VI) is adsorbed as  $\text{HCrO}_4^-$  on TTCNS under highly acidic conditions, since the surface is highly protonated. The reason for the non-interference of these cations over Cr(VI)-TTCNS system may be due to electrostatic repulsion between the cations and the positively charged surface of the adsorbent. Similar results were reported by Suresh Gupta et al.,<sup>229</sup> for  $\text{Ca}^{2+}$  and  $\text{Mg}^{2+}$  interference.

In case of Cr(VI)–TAINS system, as the concentration of these cations increased between 11 to 100 ppm, the uptake of Cr(VI) ions by TAINS was hindered, but only to a smaller extent. The influence of these ions on Cr(VI) uptake onto both the adsorbents were less significant compared to other metal ions discussed in chapters IV and V.

## 6.8 Effect of Anions

Of all the anions' ( $\text{NO}_3^-$ ,  $\text{Cl}^-$  and  $\text{SO}_4^{2-}$ ) interferences for Cr(VI)-TTCNS system, the presence of nitrate has very minimal retarding effect on its removal (Fig.6.19). The presence of  $\text{Cl}^-$  and  $\text{SO}_4^{2-}$  decreases the sorption of Cr(VI) to a certain extent. The inhibiting effect of chloride on Cr(VI)-TAINS system was less (Fig. 6.22) compared to  $\text{SO}_4^{2-}$  similar to the findings of Xue Song Wang et al.,<sup>132</sup>. The reason being, divalent  $\text{SO}_4^{2-}$  ion competes more for the adsorption sites with  $\text{HCrO}_4^-$  ions rather than  $\text{Cl}^-$  and  $\text{NO}_3^-$  ions. Such type of inhibition effect has been reported for the Cr(VI) removal on surfactant modified coconut coir pith<sup>191</sup>.

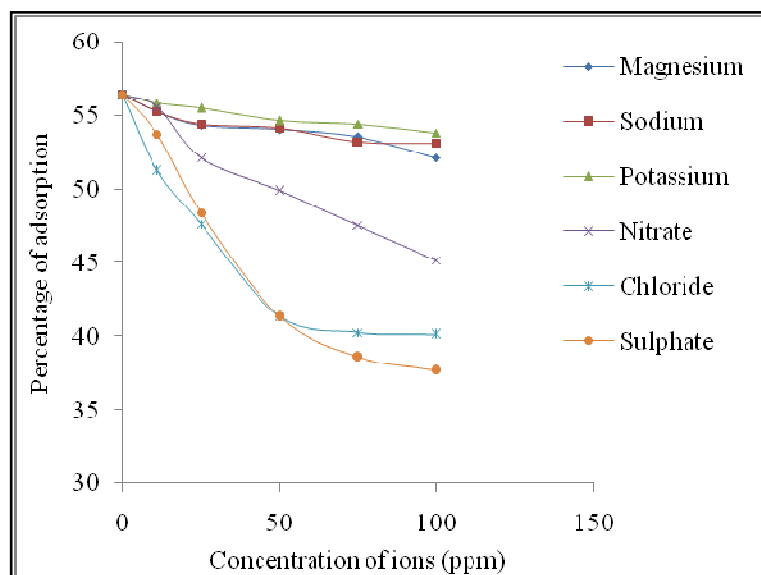


**Figure 6.19 Effect of Cations and Anions (TTCNS)**

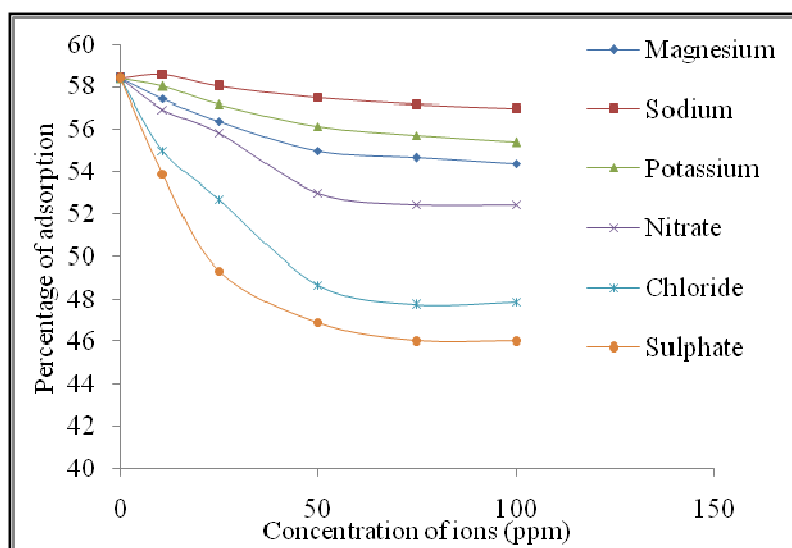


**Figure 6.20 Effect of Cations and Anions (TAINS)**

### 6.9 Effect of Co-ions

The influence of divalent co-ions on Cr(VI)-TTCNS & TAINS were meager to about 2 to 4.5% (Figures 6.21 and 6.22). Maximum Cr(VI) adsorption onto the employed adsorbents occurred at low pHs of 1.78 and 1.98 respectively. At low pHs, the protonation of

the surface plays an important role in adsorption of Cr(VI), thus prohibiting the interference of Ni(II) and Co(II) on Cr(VI) removal.

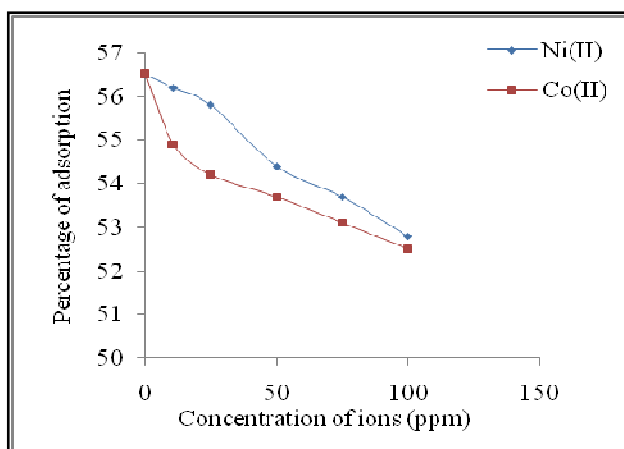


**Figure 6.21 Effect of Co- ions (TTCNS)**

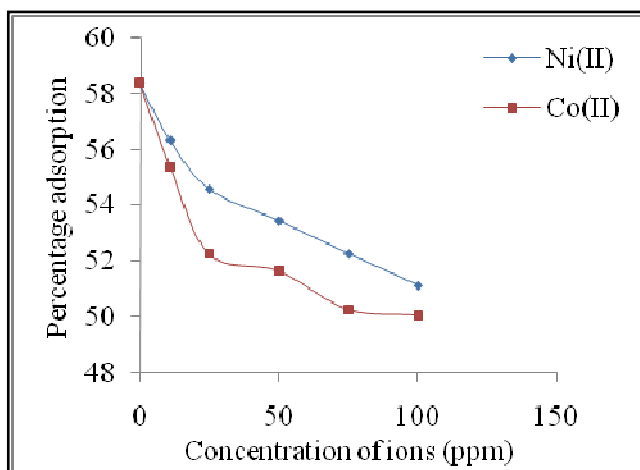


**Figure 6.22 Effect of Co- ions (TAINS)**

### 6.10 Effect of Temperature

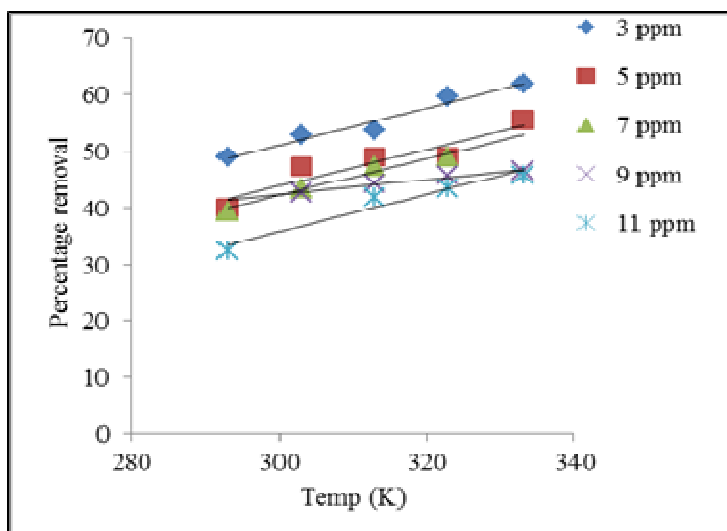
Temperature has marked effect on adsorption process. It was observed from the figures 6.23 and 6.24 that the adsorption capacities of Cr(VI) onto TTCNS and TAINS increased slightly with temperature upto 323K after which the percentage removal was not appreciable at varying initial concentrations. At 333K, a change in the texture of the

adsorbent materials might have occurred at specified pH ranges, thence reduction in sorption capacity.<sup>150</sup>

**Table 6.7 Effect of Temperature (TTCNS)**

Conc of ions (ppm)	Percentage Removal				
	293 K	303 K	313 K	323 K	333 K
3	48.9	52.8	53.63	59.63	60.00
5	40.00	47.27	48.90	48.90	51.45
7	39.45	43.36	47.27	48.90	49.63
9	37.27	42.54	44.18	45.70	46.54
11	32.36	41.81	41.89	43.36	44.72

Adsorbent dose: 200 mg; pH: 1.78; Agitation time: 30 min

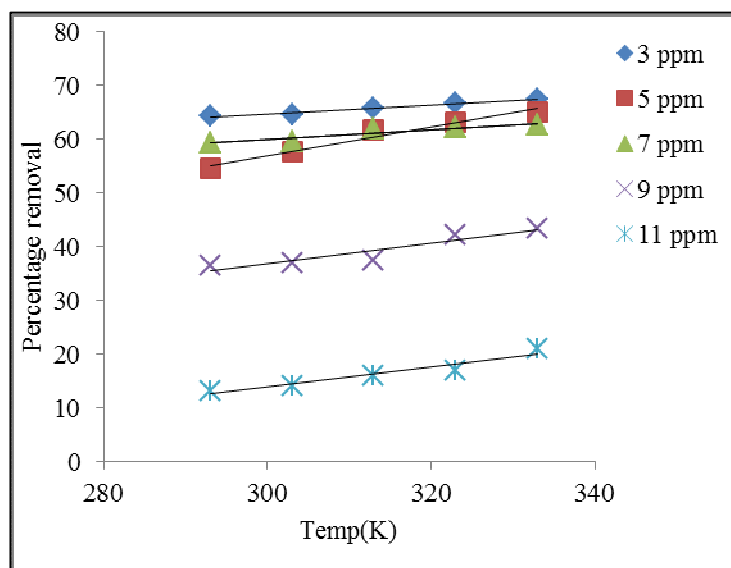


**Figure 6.23 Effect of Temperature (TTCNS)**

**Table 6.8 Effect of temperature (TAINS)**

Conc. of ions (ppm)	Percentage Removal				
	293 K	303 K	313 K	323 K	333 K
3	64.27	64.46	65.59	66.53	67.29
5	54.47	57.67	61.63	63.14	64.03
7	59.33	59.57	61.79	62.13	62.57
9	36.33	36.8	37.35	42.21	43.22
11	13.18	14.13	16.01	16.95	19.93

Adsorbent dose: 150 mg; pH: 1.98; Agitation time: 15 min

**Figure 6.24 Effect of Temperature (TAINS)**

## 6.11 Desorption

The desorption of Cr(VI) from TTCNS and TAINS were carried out at varying concentrations of HCl. Desorption efficiency of Cr(VI) is low, wherein with 1M NaOH only 14.45 % and 9.80% of Cr(VI) was desorbed from Cr(VI)-TTCNS system and Cr(VI)-TAINS systems respectively. Poor desorption confirms that the adsorption of Cr(VI) is not mostly by ion exchange mechanism. Surface complexation may contribute an important role in the adsorption. Therefore, the regeneration studies were restricted only to the metal-adsorbent systems that are discussed in chapters IV and V (Page nos.95 and 144)

## 6.12 Adsorption Isotherms

In order to determine the mechanism of Cr(VI) adsorption on TTCNS and TAINS, the experimental data were applied to Langmuir, Freundlich, Tempkin and Dubinin-Kaganer-Radushkevich isothermal equations. The constant parameters of the isotherm equation for this adsorption process were calculated by regression using linear form of the equations.

### 6.12.1 Langmuir isotherm model

The Langmuir constant  $q_m$  which is a measure of the monolayer adsorption capacity of TTCNS and TAINS towards Cr(VI) was observed as 18.6 and 10.6 mg/g and the Langmuir constant  $b$ , (free energy of sorption) was found to be 0.38 and 0.66 respectively. The correlation coefficient  $R^2$  for Cr(VI) ion with the adsorbents were found to be 0.9997 and 0.9870 respectively (Figures 6.25 and 6.26), indicating a good agreement between the experimental values and the isothermal parameters. This also confirms the monolayer adsorption of the Cr(VI) by adsorbents surface. The  $R_L$  (table 6.9) values calculated with initial concentration ranges 3-11 mg/L were between 0.47 to 0.12 ( $0 < R_L < 1$ ) which is consistent with the requirement for a favourable adsorption process.

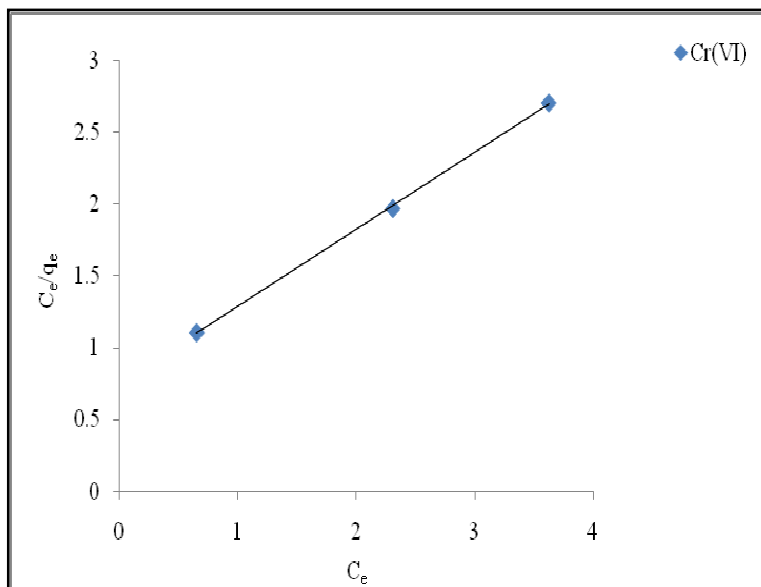


Figure 6.25 Langmuir isotherm model [Cr(VI)-TTCNS]

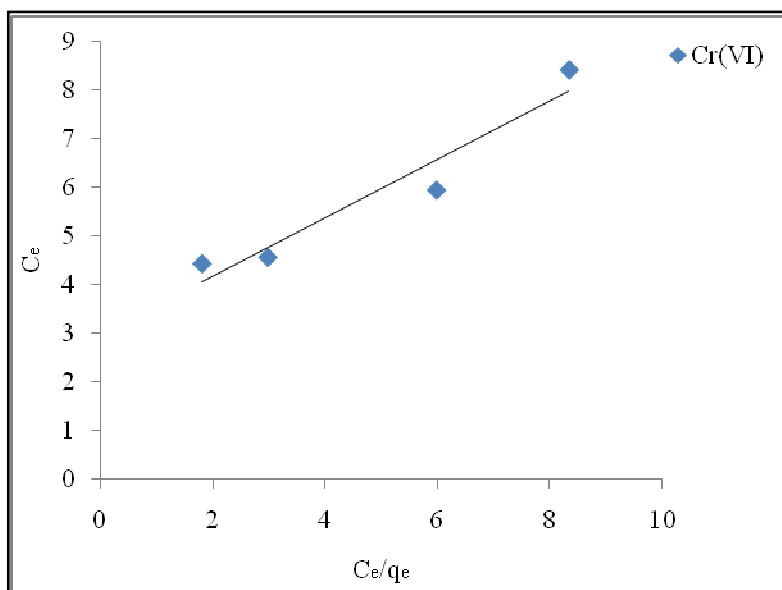


Figure 6.26 Langmuir isotherm model [Cr(VI)-TAINS]



**Table 6.9 Equilibrium parameter ( $R_L$ )**

Conc. of metal ion (mg/L)	Cr(VI)-TTCNS	Cr(VI)-TAINS
3	0.47	0.34
5	0.34	0.23
7	0.27	0.18
9	0.23	0.14
11	0.19	0.12

### 6.12.2 Freundlich isotherm model

The Freundlich plot of  $\log q_e$  versus  $\log C_e$  for the adsorption of Cr(VI) onto TTCNS and TAINS (figures 6.27 and 6.28) were employed to generate the intercept value of  $K_F$  and the slope of  $1/n$ . The figures illustrate that adsorption of Cr(VI) onto TTCNS and TAINS obeyed Freundlich isotherm very well.  $K_F$  derived from the equation (13) is an indicator of adsorption capacity of a given adsorbent. The results obtained indicate that TTCNS have higher capacity to adsorb Cr(VI) compared to TAINS. The value of 'n' greater than 1 implies favourable nature of adsorption. The TTCNS isotherm shows better linearity than the TAINS isotherm<sup>232</sup>.

**Table 6.10 Equilibrium concentrations - Freundlich isotherm**

Conc. of metal ion (mg/L)	Cr-TTCNS		Cr-TAINS	
	$\log C_e$	$\log q_e$	$\log C_e$	$\log q_e$
3	-0.187	-0.2039	0.2576	-0.3979
5	-0.301	0.0511	0.4742	-0.1739
7	0.3636	0.0689	0.7126	-0.2146
9	0.5599	0.1277	0.7767	0.004
11	0.5563	0.2636	0.9211	-0.0506

Adsorbent dose : 200mg (TTCNS), 150mg (TAINS) ; Temperature: 303K

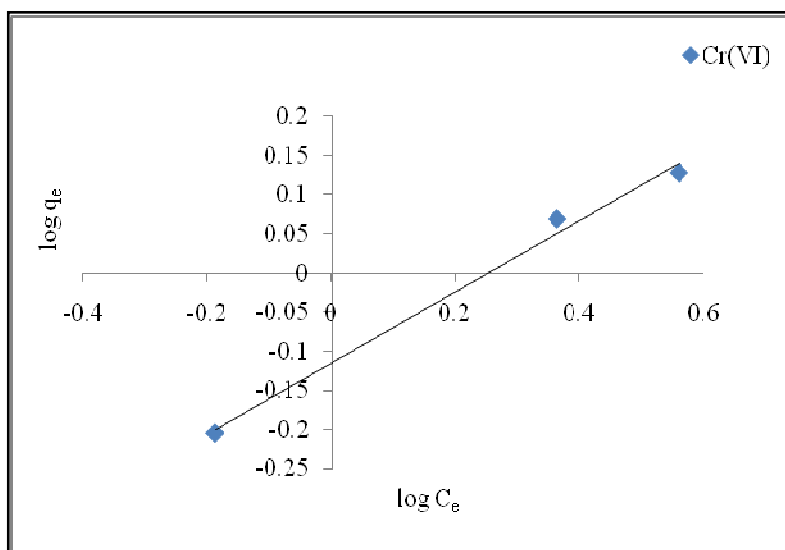


**Figure 6.27 Freundlich isotherm model [Cr(VI)-TTCNS]**

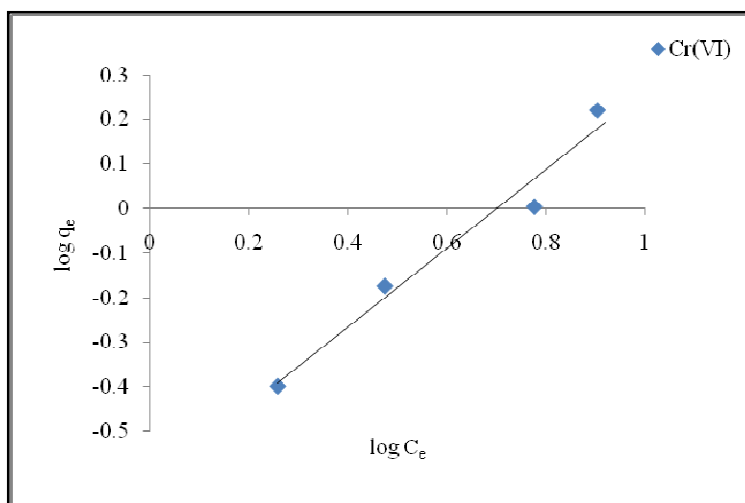


**Figure 6.28 Freundlich isotherm model [Cr(VI)-TAINS]**

### 6.12.3 Tempkin isotherm model

Tempkin isotherm was applied to the adsorption data (Table 6.11) under investigation, as per equation (14). The equilibrium binding constant  $A_T$  and heat of adsorption  $b_T$  are obtained from the slope and intercept of the linear plot of  $\ln C_e$  versus  $q_e$  (figures 6.29 and 6.30). The binding constant values 1.002 and 1.001 for the respective systems viz., Cr(VI)-TTCNS and TAINS indicate that Tempkin isotherm is obeyed by both the systems less effectively

compared to Langmuir model. Similar results were documented by Hamed Mosavian et al.,<sup>171</sup>

**Table 6.11 Equilibrium concentrations - Tempkin isotherm**

Conc. of metal ion mg/L	Cr(VI)-TTCNS		Cr(VI)-TAINS	
	$\ln C_e$	$q_e$	$\ln C_e$	$q_e$
3	-0.4307	0.5875	0.5933	0.3967
5	-0.6931	1.1250	1.0921	0.6733
7	1.1720	0.8372	1.6411	0.6133
9	1.3420	1.2892	1.7887	1.0067
11	1.8350	1.2974	2.1213	0.8867

Adsorbent dose : 200mg (TTCNS), 150mg (TAINS); Temperature: 303K

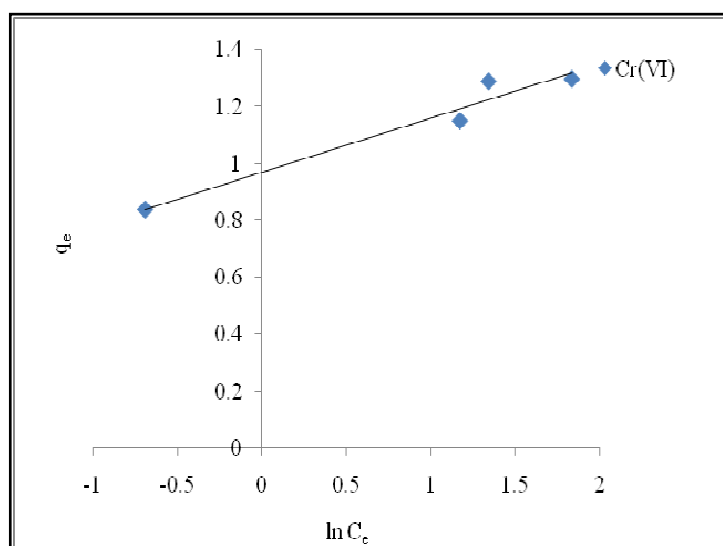


**Figure 6.29 Tempkin isotherm model [Cr(VI)-TTCNS]**

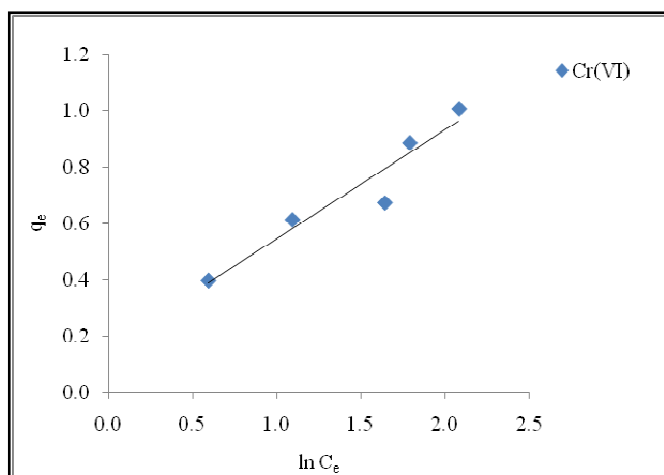


**Figure 6.30** Tempkin isotherm model [Cr(VI)-TAINS]

#### 6.12.4 DKR isotherm model

Figures.6.31 and 6.32 representing the DKR plots ( $\ln q_e$  versus  $\varepsilon^2$ ) is derived from the experimental data (table 6.12) for both the systems. The mean sorption energy calculated from the slope was 8.64 kJ/mol and 8.4 kJ/mol for the sorption of Cr(VI) onto TTCNS and TAINS respectively. The results show that the sorption of the the metal ion onto TTCNS and TAINS may be carried out via surface complexation. Similar finding were reported for various adsorbents<sup>191,286</sup>.

**Table 6.12** Equilibrium concentrations - DKR isotherm

Conc. of metal ion (mg/L)	Cr(VI)-TTCNS		Cr(VI)-TAINS	
	$\varepsilon^2 \times 10^8$	$\ln q_e$	$\varepsilon^2 \times 10^8$	$\ln q_e$
3	55.0407	-0.531	121.8872	-0.92
5	79.5921	0.117	54.3715	-0.4
7	8.1788	0.158	19.2059	-0.49
9	3.7534	0.294	15.609	0.01
11	3.7011	0.607	6.9068	-0.12

Adsorbent dose : 200mg (TTCNS), 150mg (TAINS); Temperature: 303K

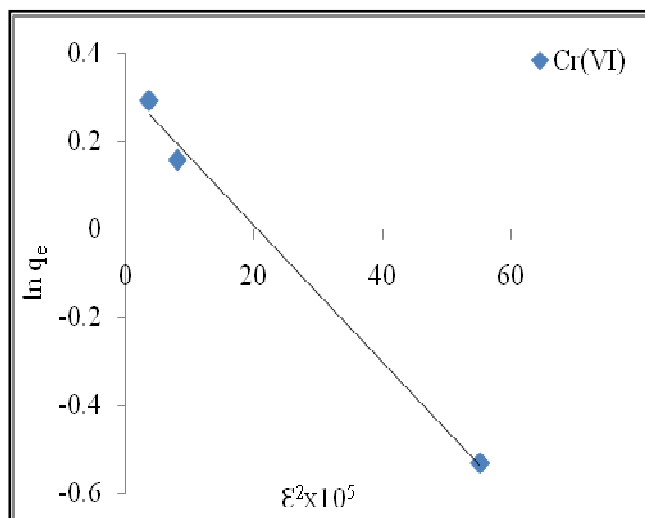


Figure 6.31 DKR isotherm model [Cr(VI)-TTCNS]

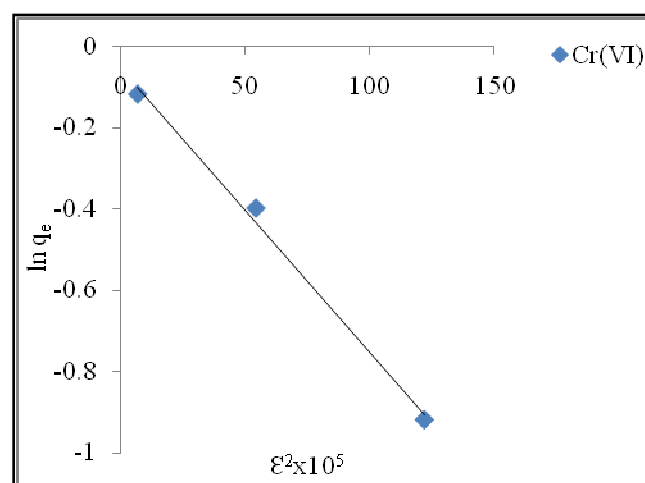


Figure 6.32 DKR isotherm model [Cr(VI)-TAINS]

### 6.13 Adsorption Kinetics

The adsorption kinetics were investigated with an aim of obtaining a deep insight into how the amount of adsorbed metal changes with time and the process time required to achieve equilibrium between the aqueous and the solid phase. The kinetics of Cr(VI) sorption onto TTCNS and TAINS were analyzed using different kinetic models such as Pseudo-first-order, Pseudo-second-order, Elovich and intraparticle diffusion models.

### 6.13.1 Pseudo-first-order model

The pseudo-first-order rate expression of equation (18) was used to test the experimental data for Cr(VI) onto TTCNS and TAINS are tabulated in tables 6.13 and 6.14 respectively. The values of  $k_1$ , pseudo-first-order rate constant and  $q_e$  calculated obtained by the plot of  $\log(q_e - q_t)$  versus  $t$  are presented in table 6.18 with coefficients of regression and SSE.

**Table 6.13 Effect of concentration-Kinetics [Cr(VI)-TTCNS]**

Time (min)	3 (ppm)		5 (ppm)		7 (ppm)		9 (ppm)		11 (ppm)	
	$\log(q_e - q_t)$	$t/q_t$	$\log(q_e - q_t)$	$t/q_t$	$\log(q_e - q_t)$	$t/q_t$	$\log(q_e - q_t)$	$t/q_t$	$\log(q_e - q_t)$	$t/q_t$
5	0.8721	1.1620	1.176	0.6660	1.053	0.4115	1.07	0.3311	1.1122	0.2105
10	0.5118	1.1760	0.942	0.7272	0.6901	0.5390	0.5378	0.4273	0.9566	0.3616
15	0.3979	1.6210	0.8162	0.9404	0.6812	0.8402	0.5118	0.6355	0.826	0.5000
20	0.2304	1.9900	0.574	1.0660	0.243	0.9216	0.4842	0.8403	0.716	0.6557
25	0.0413	2.3470	1.1172	1.2880	-0.3467	1.0869		0.9671	0.4149	0.7122
30		2.5530		1.3330		1.2793		1.1173		0.8174

Adsorbent dose: 200 mg; pH: 1.78; Temperature: 303K

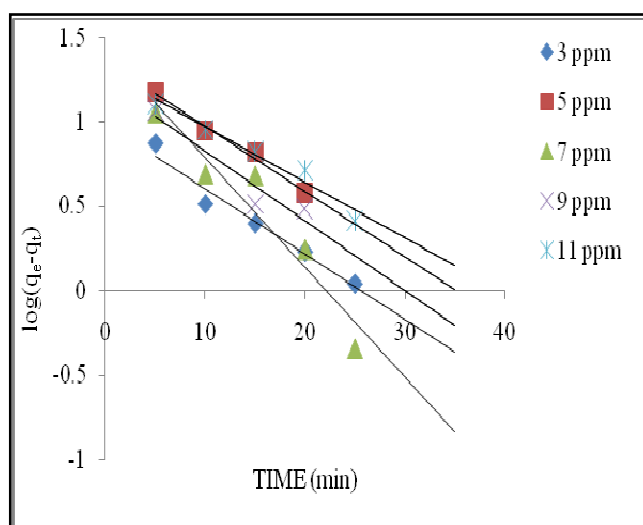


**Figure 6.33 Pseudo-first-order kinetics [Cr(VI)-TTCNS]**

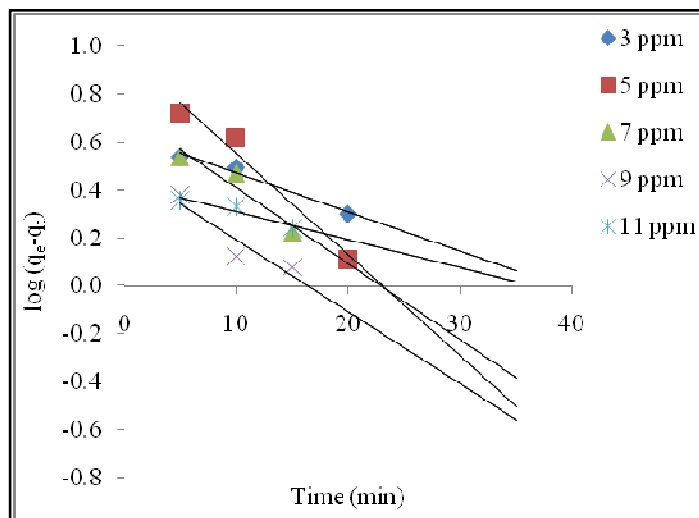


**Figure 6.34 Pseudo-first-order kinetics [Cr(VI)-TAINS]**

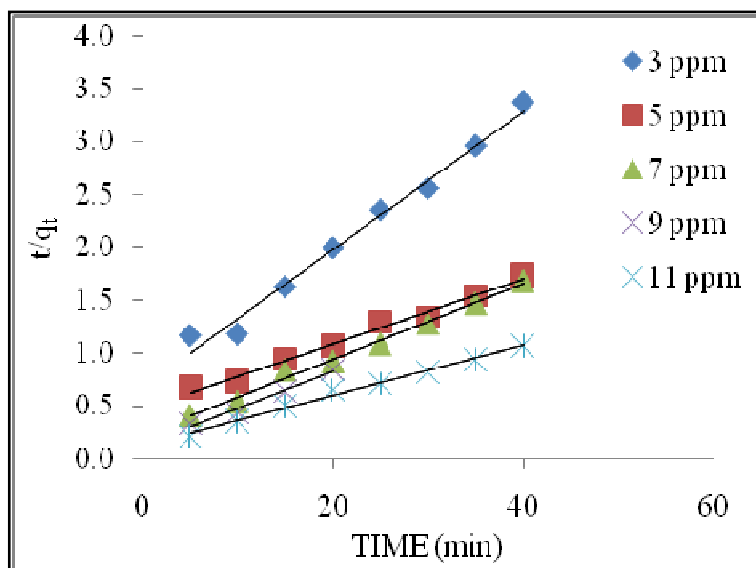
### 6.13.2 Pseudo-second-order model

The values of pseudo-second-order rate constants obtained by the plot of  $t/q_t$  versus  $t$  (figures 6.35 & 6.36) are presented in table 6.15 with coefficients of regression and SSE. The  $R^2$  values observed for pseudo-second-order model were greater than the other employed systems. The decrease in  $K_2$  and increase in  $q_e$  values with an increase in metal concentration was observed. The increase in  $q_e$  with concentration may be due to the more efficient utilization of the sorptive capacities of the adsorbents due to greater driving force (by a higher concentration gradient pressure)<sup>142</sup>. As the increase in the metal concentration reduced the diffusion of metal ions in the boundary layers,  $K_2$  decreased with concentration<sup>282</sup>.

**Table 6.14 Effect of concentration-Kinetics [Cr(VI)-TAINS]**

Time (min)	3 (ppm)		5 (ppm)		7 (ppm)		9 (ppm)		11 (ppm)	
	log (q <sub>e</sub> -q <sub>t</sub> )	t/q <sub>t</sub>	log (q <sub>e</sub> -q <sub>t</sub> )	t/q <sub>t</sub>	log (q <sub>e</sub> -q <sub>t</sub> )	t/q <sub>t</sub>	log (q <sub>e</sub> -q <sub>t</sub> )	t/q <sub>t</sub>	log (q <sub>e</sub> -q <sub>t</sub> )	t/q <sub>t</sub>
5	0.5385	1.2394	0.7236	0.8133	0.5372	0.6762	0.3793	0.3951	0.3554	0.3695
10	0.4941	2.2882	0.6180	1.3716	0.4676	1.2651	0.1238	0.7289	0.3291	0.7317
15	0.4618	3.2649	0.5174	1.8408	0.2203	1.6341	0.0781	1.0828	0.2389	1.0664
20	0.3008	3.6424	0.1107	1.9705	-0.1929	1.9610	-0.8822	1.3406	-0.8751	1.2766
25		3.9839	-2.3310	2.3148	-2.4534	2.3070		1.6609		1.5823
30		4.0053	-2.3310	2.6234		2.5578		1.8926		1.8750
35		4.6618		3.0347		2.9330		2.1967		2.1429
40		5.0279		2.9770		3.2685		1.9888		2.2556

Concentration:3-11 mg/L; Adsorbent dose: 150 mg; pH: 1.98; Temperature: 303K

**Figure 6.35 Pseudo-second-order kinetics [Cr(VI)-TTCNS]**



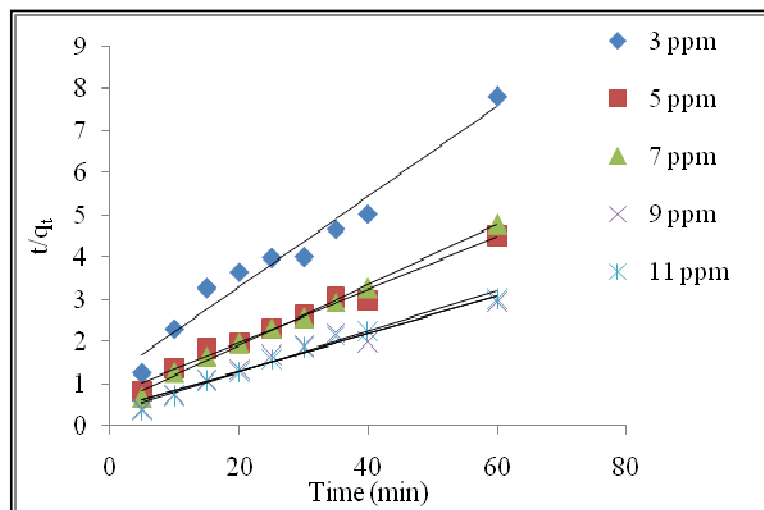


Figure 6.36 Pseudo-second-order kinetics [Cr(VI)-TAINS]

Table 6.15 Pseudo-first-order and Pseudo-second-order kinetic constants at different concentrations

Conc. of metal ions (mg/L)	$q_e$ exp. (mg/g)	Pseudo-first-order kinetics				Pseudo-second-order kinetics			
		$q_e$ cal. (mg/g)	$k_1 \times 10^{-2}$ (min <sup>-1</sup> )	$R^2$	SSE	$q_e$ cal. (mg/g)	$k_2 \times 10^{-3}$ (g/mg min)	$R^2$	SSE
<b>Cr(VI)-TTCNS</b>									
3	11.75	9.80	8.90	0.9625	0.87	15.31	6.3	0.9860	1.25
5	22.50	22.90	8.88	0.9866	0.20	32.47	2.0	0.9878	3.52
7	23.45	27.41	14.94	0.9155	1.77	27.93	5.7	0.9922	1.58
9	26.85	17.43	9.53	0.9173	4.71	28.82	0.97	0.9766	0.69
11	36.70	19.70	7.53	0.9622	7.60	42.37	0.43	0.9908	2.00
<b>Cr(VI)-TAINS</b>									
3	6.28	4.31	3.75	0.9756	0.29	9.35	10.0	0.9627	1.08
5	11.44	9.49	9.74	0.9709	1.12	15.90	5.6	0.9828	1.57
7	10.84	5.30	7.30	0.9051	3.19	13.99	10.8	0.9955	1.11
9	15.05	3.12	6.93	0.8608	6.88	22.08	5.4	0.9547	2.48
11	29.60	20.65	2.69	0.9090	5.16	22.03	11.6	0.9894	2.67

### 6.13.3 Elovich model

The Elovich plots for Cr(VI)-TTCNS and Cr(VI)-TAINS systems are shown in figures 6.37 and 6.38 respectively. The kinetic constants  $\alpha$  and  $\beta$  were estimated from the intercept and slope values of the plot of  $q_t$  versus  $\ln t$  and are given in table 6.16. The constant  $\beta$ , desorption constant related to the extent of the surface coverage decreased for both the adsorbents system. The initial adsorption rate constant  $\alpha$ , increased but not regularly with concentrations for Cr(VI) systems.

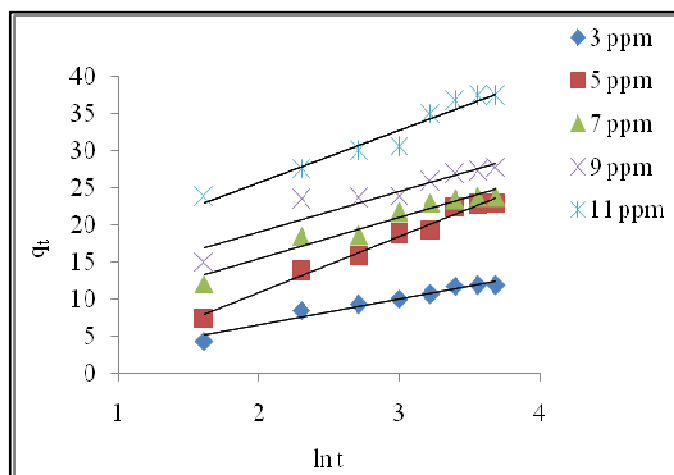


Figure 6.37 Elovich model [Cr(VI)- TTCNS]

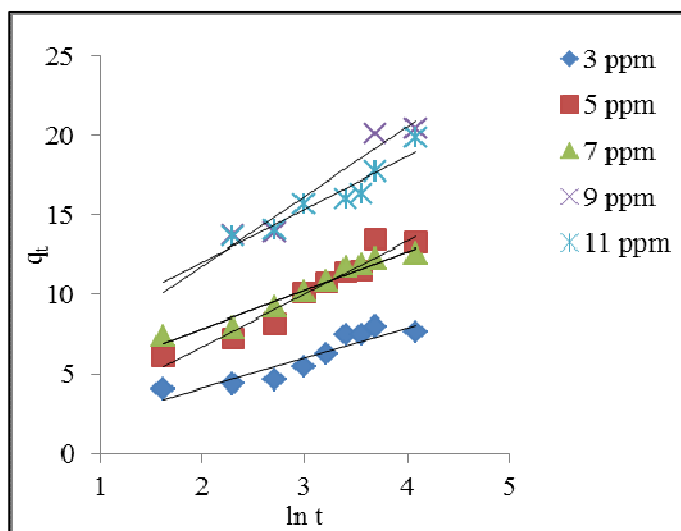


Figure 6.38 Elovich model [Cr(VI)-TAINS]

**Table 6.16 Elovich constants**

Conc. of metal ions	Cr(VI)-TTCNS			Cr(VI)-TAINS		
	$\alpha$	$\beta$	$R^2$	$\alpha$	$\beta$	$R^2$
3	1.07	0.28	0.9548	1.08	0.78	0.8553
5	1.38	0.18	0.9868	1.58	0.52	0.9427
7	1.51	0.17	0.9466	1.76	0.41	0.9510
9	2.98	0.14	0.8981	2.25	0.30	0.9379
11	3.38	0.13	0.9532	2.86	0.23	0.9032

$\alpha$  : (mg/g min),  $\beta$  : (g/mg)

#### 6.13.4 Intraparticle diffusion model

The Weber and Morris intraparticle diffusion plots which has two distinct portions<sup>280,263</sup> are presented in figures 6.39 and 6.40. The first linear portion refers to the boundary layer diffusion effect while the second linear portion refers to gradual adsorption stage, where intraparticle diffusion was rate limiting. The  $K_i$  (intraparticle rate constant) and  $C$  (boundary layer thickness) values obtained from the slopes and intercepts of linear plots of  $q_t$  versus  $t^{1/2}$  at different concentrations are shown in table 6.17. The  $K_i$  and  $C$  increased with metal ion concentration.

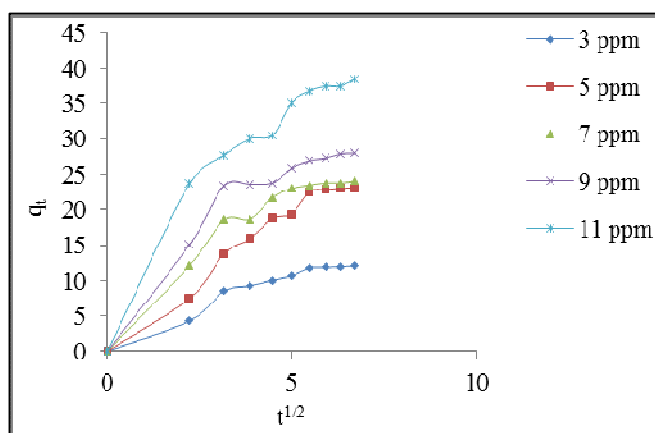


**Figure 6.39 Intraparticle diffusion model [Cr(VI)-TTCNS]**

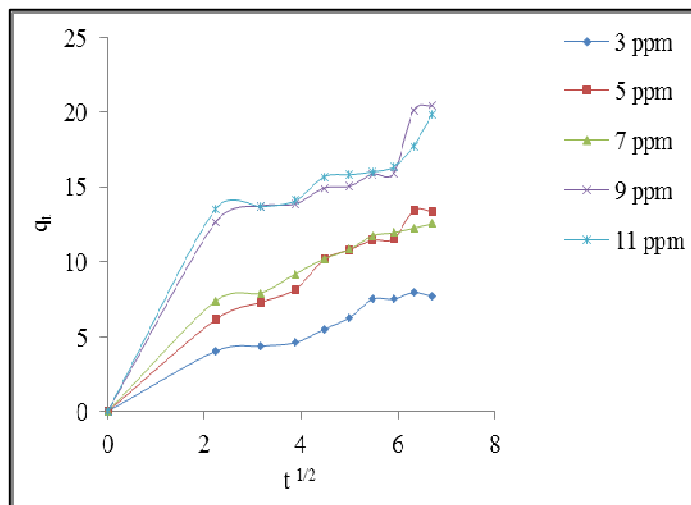


Figure 6.40 Intraparticle diffusion model [Cr(VI)-TAINS]

Table 6.17 Intraparticle diffusion model constants

Conc. of metal ions (mg/L)	Cr(VI)-TTCNS			Cr(VI)-TAINS		
	$k_i$ (mg/g min <sup>1/2</sup> )	C	R <sup>2</sup>	$k_i$ (mg/g min <sup>1/2</sup> )	C	R <sup>2</sup>
3	1.88	0.85	0.9344	1.15	0.54	0.9595
5	3.66	1.06	0.9682	1.73	0.88	0.9780
7	3.48	3.87	0.8975	1.95	1.83	0.9313
9	3.87	5.42	0.8621	2.35	3.37	0.8605
11	5.26	6.96	0.8959	2.51	4.11	0.8229

#### 6.14 Adsorption Dynamics

The thermodynamic parameters  $\Delta H^0$ ,  $\Delta S^0$  calculated from the slope and intercept of Vant Hoff plots (figures 6.41 and 6.42) are shown in table 6.18. The positive values of  $\Delta H^0$  indicate the presence of an energy barrier in the adsorption process which is endothermic in nature<sup>132</sup>. The negative values of  $\Delta G^0$  indicate the feasibility and spontaneous nature of adsorption of metal ions by the adsorbent<sup>279</sup>. The positive values of  $\Delta S^0$  suggest that the

increased randomness at the solid-solution interface during the adsorption of Cr(VI) in aqueous solutions onto TTCNS and TAINS<sup>256</sup>.

**Table 6.18** Thermodynamic constants

Temp. K	Cr(VI)-TTCNS			Cr(VI)-TAINS		
	$-\Delta G \times 10^{-3}$ kJ/mol	$\Delta H$ kJ/mol	$\Delta S$ J/mol K	$-\Delta G \times 10^{-3}$ kJ/mol	$\Delta H$ kJ/mol	$\Delta S$ J/mol K
293	4.82			1.79		
303	4.13	39.89	36.54	1.32	14.05	47.76
313	3.88			0.72		
323	0.63			0.33		
333	0.53			0.01		

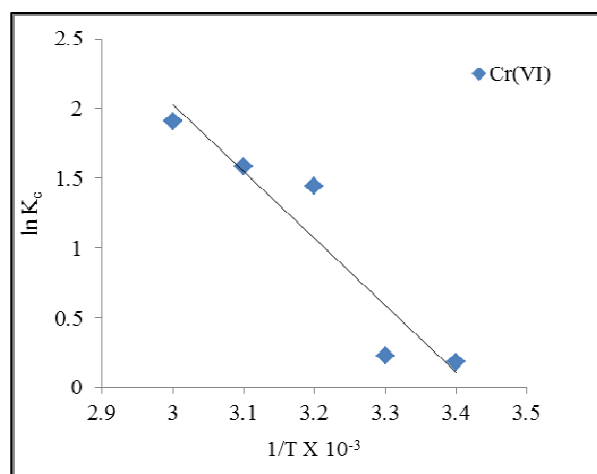


**Figure 6.41** Vant Hoff's plot [Cr(VI)-TTCNS]

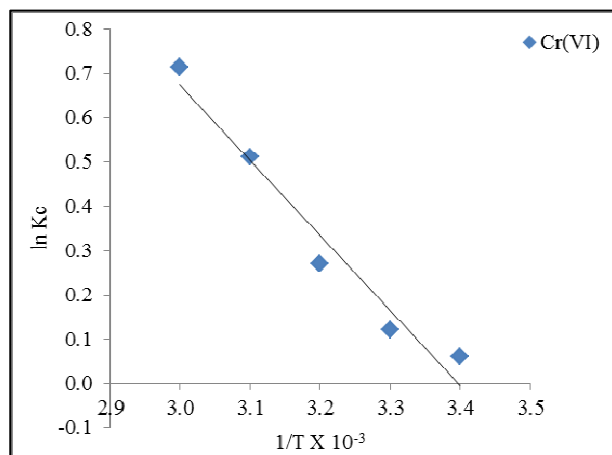


**Figure 6.42 Vant Hoff's plot [Cr(VI)-TAINS]**

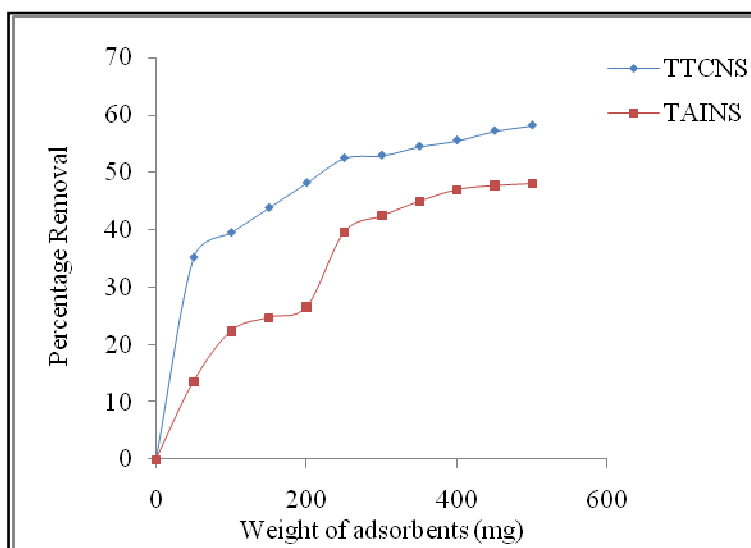
### **6.15 Effect of TTCNS and TAINS dosage on industrial effluent containing chromium**

The industrial effluent sample collected from Chromium plating industry was diluted thrice and a volume of 50 ml was employed for the batch study. The efficiency of the selected adsorbent materials on the effluent was analyzed at different adsorbents' dose at a contact time of 30 minutes by batch study. The effluent pH was adjusted to nearly 2.0 for Cr(VI) as low pH favoured Cr(VI) removal. The experimental data and the corresponding graph are shown table 6.19 and figure 6.43. A dosage of 450 mg of TTCNS and 250 mg TAINS was sufficient for the removal of Cr(VI) ( $\approx 50\%$ ), proving the sorption efficiency of the selected sorbents in treating the effluents.

**Table 6.19 Effect of TTCNS and TAINS on industrial effluent containing Chromium**

Weight of adsorbent (mg)	Percentage removal of Cr(VI) from effluent	
	TTCNS	TAINS
50	35.20	13.60
100	39.51	22.33
150	43.83	24.67
200	48.17	26.54
250	52.47	39.51
300	52.93	42.35
350	54.50	44.89
400	55.53	46.92
450	57.20	47.62
500	58.17	47.94

Particle size: 0.18mm TTCNS, 0.42 mm TAINS Agitation time: 30 minutes

**Figure 6.43 Effect of TTCNS and TAINS on effluent containing Chromium**